Proceedings of the 11th ICPMG 2026
11th International Conference on Physical Modelling in Geotechnics
8-12 June 2026, Zurich, Switzerland

A Physical Modelling Study of Cement Slurry Injection in Helical Piles Installed in Cohesive and Granular Soils

T. S. O. Morais
University of São Paulo, São Carlos, Brazil, tsomorais@sc.usp.br

O. L. L. López, C. H. C. Tsuha
University of São Paulo, São Carlos, Brazil, o.laurani@usp.br, chctsuha@sc.usp.br

ABSTRACT: Helical piles with cement injection provide an innovative foundation solution, allowing their application in soil conditions traditionally considered unsuitable for conventional helical piles. This technique allows the piles to meet design criteria such as allowable loads and displacements even in low-capacity soils where competent strata are located at considerable depths. Although cement slurry injection enhances the properties of soil disturbed during installation, the slurry flow path and its final spatial distribution within the surrounding soil remain insufficiently understood. This study enables qualitative visualization of the cement slurry flow trajectory above the helical plates through 1g physical modelling. For this investigation, reduced-scale helical pile models were installed in cohesive and cohesionless soils (soft clay and loose sand). Following cement slurry injection, the models were carefully excavated to enable direct observation of the slurry distribution within the soil mass. The qualitative visual observations indicate that, under identical injection procedures and slurry properties, cement slurry dispersion is predominantly governed by soil type. Overall, the results enhance understanding of the reinforced soil zone formed around the helical plates and contribute to the formulation of predictive hypotheses for the load-bearing capacity of cement-injected helical piles.

1 INTRODUCTION

Helical piles are steel foundation systems composed of one or more helices welded to a central shaft and installed into the ground by applying continuous torque at the pile head using hydraulic motors. This installation process disturbs the soil above the helices, potentially reducing the pile's uplift performance and overall load-bearing capacity.

The extent of installation effects depends on both soil type and pile configuration, representing a significant technical challenge for designers. For instance, Brazilian unsaturated tropical soils formed through intense weathering often exhibit high porosity and a cemented natural structure, with strength largely determined by the microstructure inherited from the parent rock. During helical pile installation, the advancement of the helices can disrupt this structure, induce soil collapse, and create voids around the shaft, thereby reducing shaft friction and compromising the pile's uplift performance (Sanchez, 2014; Tsuha et al., 2016; Santos Filho, 2019; Santos Filho & Tsuha, 2020). Mansour and El Naggar (2021) further noted that pile installation generates torsion, vertical shear, sand displacement, and stress changes, while the rotation of the pile can weaken the sand in the helix zone.

In some applications, achieving the design capacity requires the helical pile to penetrate low-strength soil layers and reach more competent strata, which may, in certain cases, necessitate large installation depths and render this foundation solution economically unfeasible. To address this limitation, helical piles with cement injection have been developed to improve pile performance and enable their use in a wider range of soil conditions.

Specifically, helical piles with cement injection enable installation in soil profiles with low bearing capacity or allow a reduction in pile length in more favourable soil conditions, due to soil improvement in the region surrounding the helical plates (Santos Filho, 2019; Santos Filho & Tsuha, 2020). However, although cement injection enhances the soil disturbed during installation, uncertainties remain regarding the slurry's flow path and its final distribution within different soil types. To better understand the mechanisms governing the performance of cement-injected helical piles, the present study reports a qualitative visual investigation, employing 1g physical modelling in cohesive and granular soils (clay and sand).

2 INJECTED HELICAL PILES

The diffusion of cement slurry within the soil may occur through three main mechanisms: permeation, compaction, and fracturing, each serving specific purposes and requiring distinct equipment for execution (Mitchell, 1982; Winterkorn & Pamukcu, 1990; Brown, 2001). Diffusion by permeation occurs when the fluid penetrates and fills the soil pores. In the compaction mechanism, the injected fluid occupies existing voids and induces compression of the surrounding soil. In the fracturing mechanism, the soil is fractured under high injection pressures, and the injection fluid does not permeate the porous medium (Mitchell, 1982; Winterkorn & Pamukcu, 1990). According to Zhang et al. (2020), the diffusion mechanism of the injection fluid in soil may transition from permeation to compaction, and from compaction to fracturing, as the soil's effective diameter, D_{10} (defined as the diameter through which 10% of the total soil mass passes), decreases and as the injection pressure increases.

In sites with soil profiles that exhibit abrupt transitions between low-strength soils and highly resistant soils or rock, conventional helical piles often become technically and economically unfeasible. Injection-based helical pile solutions have been progressively developed and documented in the technical literature (Manke, 2004; Nasr, 2008; Sanchez, 2014; Santos Filho, 2019; Santos Filho & Tsuha, 2020; Mansour & El Naggar, 2021; Santos Filho et al., 2023, 2024; Mahdavi & Lehane, 2025).

In Brazil, the first field study involving injected helical piles was conducted by Sanchez (2014). The pioneering results, based on a comparison between conventional and injected multi-helix helical piles installed in silty–clayey–sandy residual soil, demonstrated that the uplift capacity of the injected piles was 104% higher than that of the conventional piles. Additionally, the study showed that the injected cement slurry effectively filled the voids created by the passage of the helices during installation. Subsequently, Santos Filho (2019) developed two new procedures for cement slurry injection from within the helical pile, carried out at the end of installation through holes drilled in the central shaft near the helices. The first procedure involves simple injection, using a specialized sealing system at the connections between the pile components (Figure 1a). The second employs an inflatable packer to enhance the performance of the reinforced zone around the helices (Figure 1b). Brazilian studies on injected helical piles have primarily involved full-scale field tests using helical pile elements typical of power transmission line tower foundations, including shaft thickness, number of helices, and helix diameters, as reported by Santos Filho & Tsuha (2020) and Santos Filho et al. (2023). Figure 2a illustrates the installation of injected helical piles at a 525 kV self-supporting tower, while Figure 2b shows the configuration of the equipment used for cement slurry injection in these Brazilian investigations.

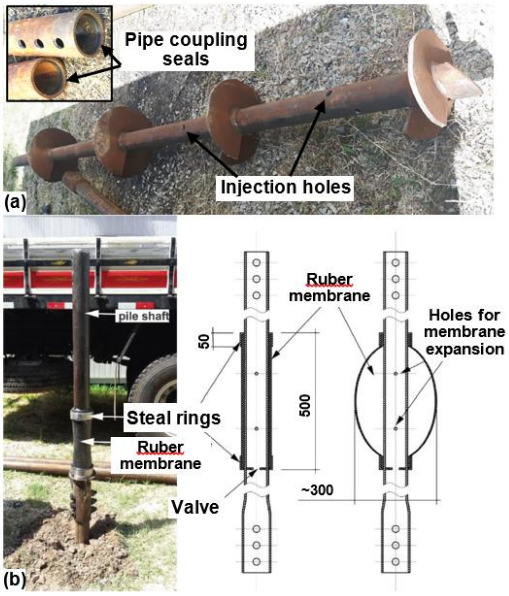

Figure 1. Cement-injected helical piles in Santos Filho (2019): (a) pile with injection holes near the helices; (b) pile with an inflatable packer, before and after expansion.

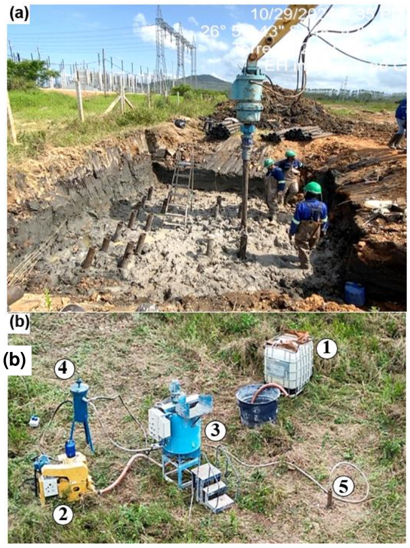

Figure 2. Injected helical pile: a) installation pile group in the field; b) cement grout injection equipment:(1) water reservoir, (2) piston pump, (3) grout mixing tank, (4) pressure stabilizer, (5) injection shutter coupled to the pile.

3 PHYSICAL MODELING

Field exhumation of full-scale cement-injected helical piles poses significant technical and logistical challenges, highlighting the value of reduced-scale physical modelling for investigating slurry-soil interactions. 1g model tests provide a cost-effective and controlled approach to: (i) directly visualize the cement slurry flow path, (ii) assess the influence of soil conditions and pile configuration, and (iii) ensure experimental repeatability. Reduced-scale helical pile models were utilized in this study to evaluate cement slurry injection, with particular focus on the soil region above the helices. Two characteristic soil types were considered: loose sand and soft clay.

3.1 Model pile and pile installation system

For this study, reduced-scale (1:10) triple-helix pile models were fabricated to enable a qualitative evaluation of cement slurry geometry. Each model pile consists of a lead section equipped with three helical plates (H1 to H3, Figure 3b) of increasing diameters (25.4 mm, 30.5 mm, and 35.6 mm), spaced at three times the helix diameter (76.2 mm and 91.5 mm) along a circular shaft. This configuration is representative of helical pile types commonly used in the foundations of transmission line towers in Brazil. Figure 3 illustrates the construction of the injected helical pile models, while Table 1 summarises their dimensions and geometric characteristics.

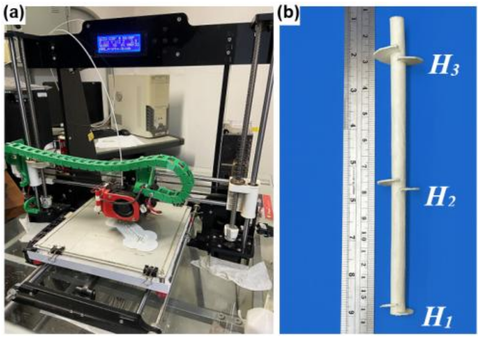

Figure 3. (a)3D Printing of helical pile models; (b) pile lead section with helix nomination.

Table 1. Pile model dimensions (mm).

Lead section length	200	Helix pitch	7.5
Shaft – outer diameter	10.2	H1 diameter	25.4
Shaft – thickness	1	H2 diameter	30.5
Plates – thickness	1	H3 diameter	35.6

Helical pile models were fabricated from ABS (Acrylonitrile Butadiene Styrene) thermoplastic filament, offering mechanical and thermal properties appropriate for this small-scale qualitative visual study. The helical plates interacted with the soil in a manner analogous to field installation, producing disturbance patterns replicated in the current model tests. A tubular extension sleeve made of PLA (Polylactic Acid), measuring 120 mm in length, was manufactured to be coupled to each pile model. Figure 4a shows the final configuration of the helical pile model.

Injection holes were drilled along the central axis of the lead section to allow the release of cement slurry from within the pile. As illustrated in Figure 4b, a total of eight injection holes were provided, with four located immediately above H1 and four above H2, following the configuration adopted in previous full-scale studies of injected helical piles (Santos Filho, 2019; Santos Filho & Tsuha, 2020; Santos Filho et al., 2023; Santos Filho et al., 2024).

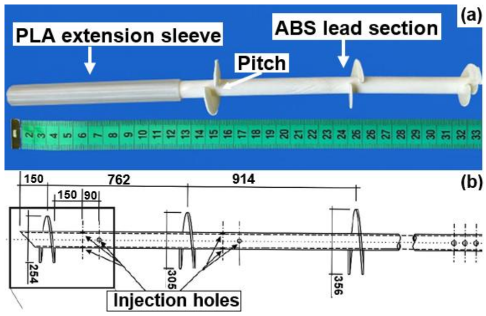

Figure 4. (a) Helical pile model; b) Prototype 3-helix lead section and injection holes (Santos Filho et al., 2023).

Installation of the helical pile model was performed by screwing the pile into the soil through the application of torque (manually) at the top of the central shaft, combined with a controlled downward vertical displacement (Figure 5).

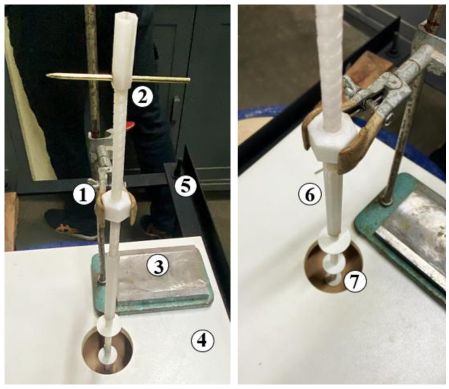

Figure 5. Manual installation system of reduced-scale helical piles: (1) hexagonal nut, (2) threaded rod, (3) laboratory support, (4) upper guide plate (5) global support frame, (6) extension sleeve and (7) 3-helix section.

The reduced-scale installation device was developed using PLA. The system comprised a 3D-printed threaded rod with the same pitch as the helical plates, a guiding hexagonal nut responsible for synchronising the rotation–penetration mechanism with each complete rotation, and a global support frame mounted on a laboratory clamp. This configuration ensured that the model pile advanced vertically by one pitch per full rotation during installation.

3.2 Soil models

To evaluate the geometry of the cement grout within the soil samples, two non-cohesive soils were used: a fine sand (Sand 1) and a medium-to-coarse sand (Sand 2). For the cohesive soil samples, three materials were selected to represent a soft clay profile with low bearing capacity: two silty–sandy clays (Clay 1 and Clay 2) and one silty–clayey soil (Silt 1). Laboratory characterization of the soil samples employed in the model tests was conducted following established Brazilian standards. The testing program included particle-size analysis, determination of the specific gravity of soil particles, maximum and minimum void ratios, and Atterberg limits. The results are summarized in Tables 2 and 3, and the particle-size distribution curves are presented in Figure 6.

Table 2. Physical properties of the granular soil samples.

Properties	Sand (1)	Sand (2)
Clay content (%)	-	-
Silt content (%)	-	-
Sand content (%)	100.0	93.0
Pebble content (%)	-	7.0
D_{10} (mm)	0.11	0.19
Dry unit weight (kN/m³)	14.3	13.8
Particle unit weight (kN/m³)	26.2	25.7
Maximum void ratio	1,10	1.02
Minimum void ratio	0.61	0.57

Table 3. Physical properties of the cohesive soil samples.

Soil Properties	Clay (1)	Clay (2)	Silt (1)
Clay content (%)	50.0	50.0	40.0
Silt content (%)	26.0	30.0	56.0
Sand content (%)	24.0	20.0	4.0
Pebble content (%)	-	-	-
D_{10} (mm)		< 0.002	
Particle unit weight (kN/m³)	25.2	26.7	26.1
Plastic limit (%)	24.0	26.8	34.7
Liquid limit (%)	46.0	46.0	59.0

Layered soil specimens were prepared in two experimental containers: (i) a truncated conical container with a circular cross-section (0.64 × 0.51 × 0.42 m) and a total volume of 0.111 m³, used for non-cohesive soils, and (ii) a prismatic container with a rectangular cross-section (0.40 × 0.30 × 0.35 m) and a volume of 0.042 m³, used for cohesive soils. In both configurations, the reconstituted soil masses were constructed in layers under strict density control, achieved by monitoring the mass and thickness of each layer. Granular soil was deposited by controlled manual pouring in thin layers without compaction, targeting a loose state with a high void ratio (relative density values presented in Figure 10). Cohesive soil was first homogenized and conditioned at a water content between the plastic and liquid limits to achieve a soft consistency, then placed in layers with mass–thickness control to ensure the desired density. This preparation protocol aligns with the objectives of the present small-scale qualitative visual investigation.

Considering the configuration of the pile models, as well as the location of the grout injection holes, the final thickness of each stratified soil mass was defined so that each pile helix was installed within a distinct soil layer. Figure 7 illustrates the soil samples investigated in this study, and the locations of the model piles (EH and EHI) and the points (A1 to A4) at which unit weight measurements were performed. In addition, four tests using a variable-energy light dynamic penetrometer (PANDA®) were conducted in the non-cohesive soil mass (points P01 to P04 in Figure 7a), providing measurements of the dynamic tip resistance (q_d).

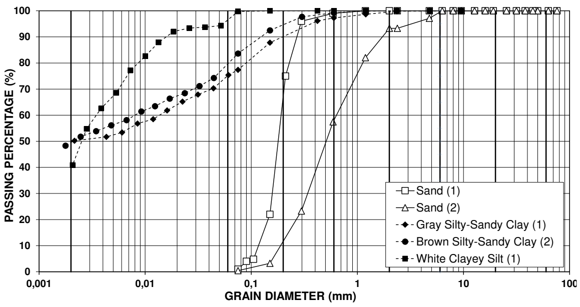

Figure 6. Particle-size distribution of soil samples.

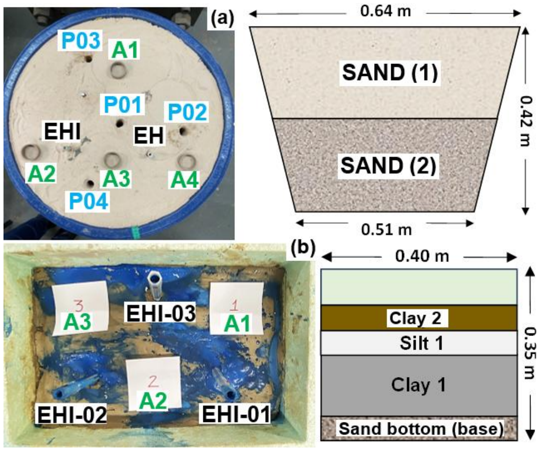

Figure 7. Layout of the soil samples (sectional view), location of the injected helical piles and investigation points (plan view): a) granular soil b) cohesive soil.

3.3 Cement slurry

The cement slurry employed in field-scale helical piles comprises a mixture of Portland–pozzolan cement and water, prepared with a predetermined water-to-cement mass ratio (w/c) of 0.5, commonly adopted for cement slurries used in the injection of soil-anchored tiebacks. This w/c ratio, combined with the use of Portland cement CP II-F 32, has been employed in field studies on injected helical piles in Brazil, as reported by Santos Filho (2019) and Santos Filho et al. (2020, 2023).

In the present study, the cement slurry was prepared using Portland cement CP II-F 32 with a water-to-cement mass ratio of 1.1:1, applied consistently to both soil types investigated. For the cohesive soil sample, a blue dye was added to the slurry to facilitate visualization of its dispersion within the clayey layers, which ranged in colour from grey (similar to the cement) to brown.

3.4 Injection and exhumation of pile models

After installation of the model piles, cement grout was injected into the soil through the holes located in the lower section of the piles (Figure 4). Prior to slurry injection, the interior of each pile shaft was flushed by injecting 60 mL of water using the same manual device later employed for the cement slurry. In all tests, this procedure eliminated soil particles potentially entering the pile during installation and cleared any blockages in the slurry outlet holes, ensuring unobstructed cement slurry discharge. Injection was then performed using a manual device with a nominal capacity of 60 mL (Figure 8). The process was carried out under volume-controlled conditions, with the injected volume monitored for each pile. Injection was terminated once cement slurry was observed overflowing at the soil surface.

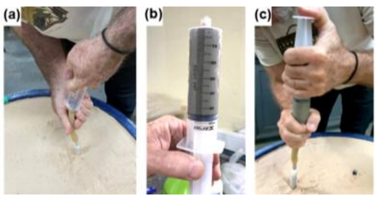

Figure 8. Cement injection procedure: a) initial cleaning with water; b) preparation of the cement slurry; c) injection of the cement slurry in the model pile.

The injected piles were exhumed manually seven days after injection. This excavation allowed determination of the natural unit weight of the soil layers adjacent to the piles at different depths. Furthermore, it enabled direct visual observation of cement slurry dispersion within the surrounding soil, providing qualitative insight into the injection process and the cement–soil interaction.

4 RESULTS AND DISCUSSIONS

4.1 Granular soil sample

In the granular soil sample, one conventional helical pile (EH) and one injected helical pile (EHI) were installed. A total of 165 mL of cement slurry was injected into the EHI, with no slurry observed at the soil surface. PANDA® tests (P01 to P04) were conducted prior to pile exhumation at the locations indicated in Figure 7a, and the resulting q_d versus depth profiles are presented in Figure 9. This figure also illustrates the spatial variability of q_d across the container plan area. All tests show an increase in q_d with depth. The highest q_d values in both layers occurred near the centre of the container, indicating higher soil densities in this region. Conversely, the lowest q_d values were recorded at P03 and P04, located closer to the EHI, suggesting comparatively lower soil densities in these areas.

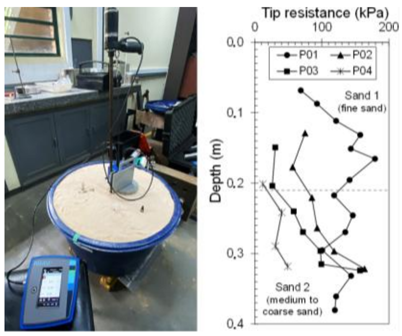

Figure 9. Dynamic tip resistance results of the sand mass.

Soil density measurements were performed during exhumation at four depths along the model pile length (0.07, 0.17, 0.28, and 0.36 m) at the plan locations A1 to A4, as shown in Figure 7a. The dry unit weight (γ_d) and relative density (D_r) results obtained from undisturbed sand samples are presented in Table 4. Figure 10 illustrates the spatial variability of D_r along a cross-section passing through points A2, A3, and A4, including the locations of the installed piles.

The results presented in Table 4, Figures 9 and 10 indicate that the piles were installed in a low-density granular soil mass, with the relative density (D_r) of Sands 1 and 2 corresponding to a very loose to medium dense sandy soil at the plan locations within the truncated conical container. Combined analysis of the γ_d measurements at A2, A3, and A4 and the PANDA® tests P2, P3, and P4 (Figure7) further shows that the installation location of the EHI coincided with the lowest soil density with depth. The exhumation of the EH and EHI piles was carried out manually and simultaneously, allowing the identification of soil disturbance caused by pile installation and the final dispersion of the cement slurry within the soil mass. Figure 11 presents the exhumation results. Figure 11a highlights the zones within the granular soil mass that experienced significant disturbance due to helical pile installation, approximately bounded by the truncated-cone region defined by the projection of the helix diameters. The disturbance was more pronounced in Sand 1 (fine loose sand), corresponding to the surface layer, which had a lower density compared to Sand 2 (medium-to-coarse loose sand). Within Sand 1, the effects of successive helix passages during installation are clearly visible, with a higher degree of disturbance observed above helix H3 compared to the zone between helices H2 and H3.

Table 4. Soil properties of the granular sample.

Depth and physical properties		A1	A2	A3	A4
0.7 m (Sand 1)	γ_d (kN/m³)	13.5	12.6	13.2	12.7
	D_r (%)	33	6	23	8
0.17 m (Sand 1)	γ_d (kN/m³)	13.3	12.4	13.3	11.8
	D_r (%)	28	0	26	5
0.28 m (Sand 2)	γ_d (kN/m³)	13.7	12.7	13.5	13.9
	D_r (%)	33	0	26	39
0.36 m (Sand 2)	γ_d (kN/m³)	13.9	14.6	14.7	13.9
	D_r (%)	37	57	59	37

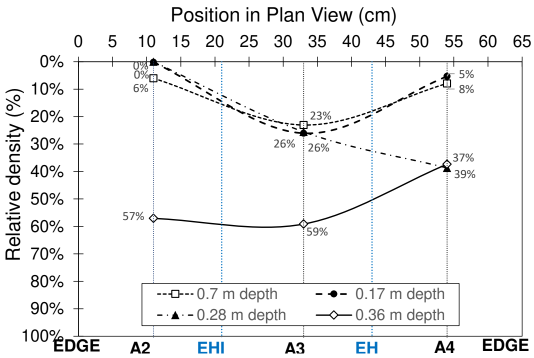

Figure 10. Spatial distribution of sand relative density (Dr) in the cross-section between points A2, A3 and A4 (shown in Figure 7).

In all zones affected by installation, downward displacement of the soil mass was observed, resulting from the dragging of sand toward the pile shaft. This effect was less pronounced between helices H1 and H2 within the Sand 2 layer, where the soil was cut only once, and more significant above helix H2 in the Sand 1 layer. The downward displacement is likely associated with a reduction in void ratio caused by helix penetration, and was most evident near the surface, where the soil had lower compactness and experienced multiple helix passages during installation.

The exhumation of the EHI (Figures 11b and 11c) revealed the formation of cement slurry bulbs adhered to the pile shaft, exhibiting varying geometries and volumes in the regions between the helices. A higher volumetric concentration of hardened slurry was observed between helices H2 and H3 (Figure 11d), corresponding to the zone where the soil was disturbed twice during installation. In this region, the slurry extended beyond the boundary defined by the helix passages, forming an oval-shaped body resembling an ellipsoidal bulb with an irregular, bulging surface (diameters: center = 46.16 mm; top = 29.42 mm; bottom = 43.18 mm). This is analogous to a clogging bulb, resulting from accumulation and adhesion of cement slurry around the shaft, likely influenced by the low soil density at the soil–foundation interface after installation in loosely compacted sand. Between helices H1 and H2, corresponding to Sand 2 and disturbed only once by H1 during installation, cement slurry adhesion to the shaft was also observed, although with a significantly smaller volume and without a well-defined geometry. Nevertheless, a tendency for slurry accumulation on the same side of the shaft identified between H2 and H3 was noted (Figure 11d), possibly due to the lower soil density in this portion of the sand mass, located between the EHI and the reservoir wall (edge).

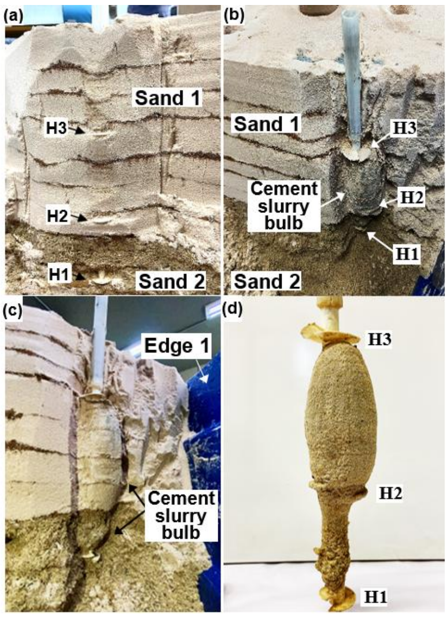

Figure 11. Exhumation of helical pile models in granular soil: a) conventional pile, b,c) injected pile, d) bulb of hardened cement slurry adhered to the model pile.

The reduced slurry accumulation between H1 and H2, despite the coarser grain size of this layer, may be attributed to: (i) a lower degree of soil disturbance during installation; (ii) a higher relative density compared with the region between H2 and H3, limiting slurry dispersion and the formation of accumulated volumes; and (iii) a greater susceptibility to blockage of the grout outlet holes in the lower section of the pile during installation.

Therefore, for the granular soils tested and the Portland cement CP II-F 32 used, no mixing of the slurry with the sand was observed in any of the bulbs, and thus no soil–cement formation by substitution occurred. Accordingly, the dispersion mechanism of the slurry in the granular soil was predominantly compaction, with no evidence of hydraulic fracturing, permeation, or substitution. The cement slurry remained homogeneous, promoting radial expansion, displacing the soil, and improving the properties previously affected by pile installation.

4.2 Cohesive soil sample

Three injected helical pile models (EHI-01 to EHI-03) were installed in the cohesive soil samples. Models EHI-01 and EHI-02 were identical, differing only in the configuration of injection outlet holes. EHI-01 was manufactured with holes located between helices H1 and H2, whereas EHI-02 had two levels of holes, consistent with the configuration adopted for the EHI tested in granular soil. Model pile EHI-03 failed during installation and was excluded from the analyses.

Following pile installation, the piles were flushed with water and subsequently injected with blue-coloured cement slurry at the same water-to-cement ratio (1.1:1). The injection sequence began with pile EHI-02. A total slurry volume of 180 mL was injected into EHI-02, while 215 mL was injected into EHI-01; in both cases, slurry extrusion was observed at the soil surface. At the end of the injection stage, uplift of the clay layers was noted, accompanied by expulsion of water from the cohesive soil mass to the surface. Additionally, slurry overflow at EHI-02 during the final stage of injection into EHI-01 indicated a possible deep hydraulic interconnection between the slurry zones. As in the granular soil sample, soil property measurements were performed during pile exhumation. In the cohesive soil mass, these measurements were taken at four depths along the model pile length (0.04, 0.10, 0.16, and 0.21 m) at plan locations A1 to A3, as shown in Figure 7a. The dry unit weight (γ_d) and average water content (w) results obtained from undisturbed samples are presented in Table 5 and the spatial variability of γ_d in Figure 12. The results of γ_d and w for the stratified cohesive soil mass indicate an increasing trend in density with depth, with position A3, located in the vicinity of EHI-02, exhibiting the lowest density. In addition, the in-situ moisture content results show that all cohesive layers presented water contents significantly higher than their respective plastic limits, with exceedances of 25% for clay 2, 52% for silt 1, and 82% for clay 1, placing them close to the liquid limit. These results confirm the soft to medium consistency condition of the analysed cohesive layers.

Figure 13 shows the cohesive soil sample, highlighting the different configurations of hardened cement slurry resulting from injection from the two model piles. In both cases, preferential slurry dispersion was observed along the interface between the Clay 1 and Silt 1 layers, indicating that stratigraphic discontinuities can act as preferential pathways for slurry propagation in low-permeability soils. This behaviour may be representative of field conditions in stratified soil profiles, particularly where fill layers overlie soft soil deposits.

Table 5. Soil properties of the cohesive sample.

Depth and physical properties		A1	A2	A3
0.04 m (Clay 2)	γ_d (kN/m³)	13.1	13.4	13.1
	w (%)		33.52	
0.10 m (Silt 1)	γ_d (kN/m³)	10.2	10.4	9.0
	w (%)		52.81	
0.16 m (Clay 1)	γ_d (kN/m³)	11.5	11.6	11.4
	w (%)		43.73	
0.21 m (Clay 1)	γ_d (kN/m³)	-	11.7	11.1
	w (%)		43.73	

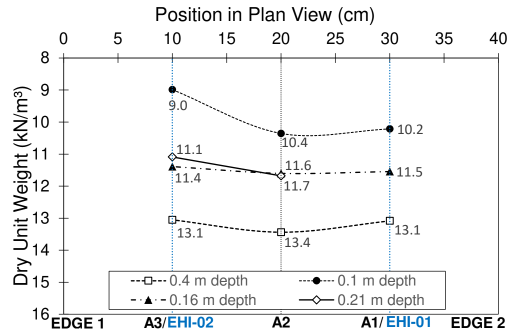

Figure 12. Probable spatial distribution of γ_d in the cross-section between points A1, A2 and A3 (shown in Figure 7).

The location of the injection holes along the pile shaft had a direct influence on the geometry of cement slurry dispersion (Figures 13b and 13c). For pile EHI-02, no slurry outflow was observed in the deeper regions near the pile tip, between helices H1 and H2, or within the Clay 1 layer (Figure 13b); slurry injection occurred only in the upper region, between helices H2 and H3, corresponding to the Silt 1 and Clay 2 layers. Helicoidal cement slurry plates, with geometry resembling helix H3, were observed exclusively within the Clay 2 layer, which has a higher clay content (≈50%), lower water content measured during exhumation and is more affected by installation. In contrast, at the depth corresponding to the Silt 1 layer (≈40% clay content and higher water content), only localized adhesion of the slurry to the pile shaft was observed.

For pile EHI-01, which had a single level of injection holes between helices H1 and H2, the slurry ascended from the Clay 1 layer and accumulated up to the interface with the Silt 1 layer. Despite the presence of the helical installation path within the Silt 1 and Clay 2 layers, no helicoidal slurry plates formed, indicating that the ascending slurry preferentially dispersed along the stratigraphic discontinuity.

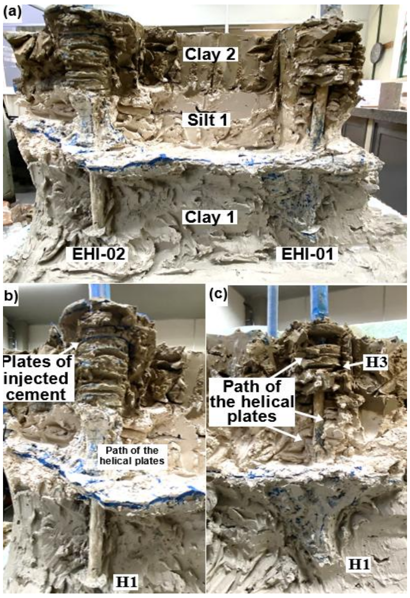

Figure 13. Exhumation of helical pile models in cohesive soil sample: a) injected pile models, b) EHI-02 and helical plates of hardened slurry cement, c) EHI-01 and the dispersion of cement slurry from the model pile tip.

5 CONCLUSIONS

The injection of cement in helical piles represents a recent advancement in foundation engineering, extending the applicability of this foundation system to low-capacity soils where conventional helical piles are typically unsuitable. Despite its potential, uncertainties remain regarding the mechanisms governing cement slurry dispersion within the soil mass. This study employs 1g physical modeling to qualitatively investigate the flow behavior of cement slurry injected through reduced-scale helical pile models in loose sand and soft cohesive soils. Slurry dispersion was shown to be governed by soil type, physical properties, stratification, and injection-hole location, revealing the formation and extent of the reinforced soil zone around the helical plates. Despite the simplified model conditions, the results provide mechanistic insights into slurry–soil interaction processes, supporting the development of predictive approaches for cement-injected helical pile performance. Key limitations include a higher water-to-cement ratio than field practice, manual slurry injection, absence of in-situ stress representation, and the soil preparation method.

ACKNOWLEDGEMENTS

The authors acknowledge the financial support provided by Neoenergia Group through the ANEEL R&D Program (Project PD-07284-0002/2020).

REFERENCES

Brown, R. W. (2001). *Pratical Foundation Engineering Handbook.* 2. ed. New York: McGraw Hill Companies, Inc., 1228 p.

Mahdavi, A., B. M., Lehane. (2025). A new grouting procedure to enhance axial response of helical piles in sand. *Proceedings of the Institution of Civil Engineers - Geotechnical Engineering*, Volume 178, Issue 5, p. 525-533, https://doi.org/10.1680/jgeen.24.00348. 2025.

Manke, J.P. 2004. *Assessment of superposition as a design framework for the combined effects of soil improvement and foundation remediation*. Master's thesis, North Carolina State University, United States.

Mansour, M. A. and M. H., El Naggar. (2021). Optimization of grouting method and axial performance of pressure-grouted helical piles. *Canadian Geotechnical Journal*. 59(5): 702-714. https://doi.org/10.1139/cgj-2021-0093

Nasr, M. H. 2008. *Method for installing a screw pile*. Application Publication, USA. Publ. No. US20080031695 A1.

Sanchez, L. H. (2014). *Avaliação de soluções alternativas para o aumento de capacidade de carga de fundações por estacas helicoidais. Evaluation of alternative solutions for increasing the load capacity of foundations using helical piles*. Master's thesis. University of São Paulo at São Carlos, Brazil, 154 p. (in Portuguese)

Santos Filho, J. M. S. M. (2019). *Análise do comportamento de fundações por estacas Helicoidais com injeção de calda de Cimento. Analysis of the Behavior of Helical Piling Foundations with Cement Grout Injection*. D.Sc. Thesis. University of São Paulo at São Carlos, Brazil, 171 p. (in Portuguese)

Santos Filho, J. M. S. M. and C. H. C., Tsuha. 2020. *Uplift Performance of Helical Piles with Cement Injection in Residual Soils. Canadian Geotechnical Journal*, 57 (9): 1335–1355. https://doi.org/10.1139/cgj-2019-0317.

Santos Filho, J. M. S. M., T. S. O. Morais, C. H. C., Tsuha. 2023. *Helical piles with cement injection in medium dense sand. International Journal of Geothecnical Engineering*, v. 17, p. 352–362. https://doi.org/10.1080/19386362.2023.2250200

Tsuha, C. H. C., J. M. S. M., dos Santos Filho; T. D. C., Santos. (2016). *Helical Piles in Unsaturated Structured Soil: A Case Study.* Canadian Geotechnical Journal 53 (1): 103–117. https://doi.org/10.1139/cgj-2015-0017,

Winterkorn, H. F.; S., Pamukcu. (1990). Soil Stabilization and Grouting. In: FANG, Hsai-Yang (ed.). *Foundation engineering handbook*. 2. ed. New York: Van Nostrand Reinhold; London: Chapman & Hall.

Zhang, J., Sc., Li, Zf., Li, L. Yang, Qs. Zang, K. Wang, Yh., Qi, J., Du, Ht., Li. (2020). Effect of Particle Size Distribution on the Grout Diffusion Pattern in Completely and Strongly Weathered Granite. *Indian Geotechnical Journal* 50: 531–539. https://doi.org/10.1007/s40098-019-00386-2.